ELSEVIER

Carbohydrate Research 337 (2002) 305–314

CARBOHYDRATE RESEARCH

www.elsevier.com/locate/carres

X-ray structure analysis of the sodium salt of beijeran

Wen Bian,[a] Rengaswami Chandrasekaran,[a,*] Kozo Ogawa[b]

[a] *Whistler Center for Carbohydrate Research, 1160 Food Science Building, Purdue University, West Lafayette, IN 47907-1160, USA*
[b] *Research Institute for Advanced Science and Technology, Osaka Prefecture University, Sakai, Osaka 559-8570, Japan*

Received 1 October 2001; accepted 28 November 2001

Abstract

The three-dimensional structure of the sodium salt of beijeran has been determined by X-ray fiber diffraction analysis. The acidic polysaccharide forms an extended twofold helix. Two chains are nestled tightly in a monoclinic unit cell of dimensions $a = 12.72$, $b = 11.41$, c (fiber axis) $= 24.62$ Å and $\gamma = 123.7°$ in an antiparallel fashion. In the crystalline lattice, helices are stacked tightly to form a thick sheet along the vertical plane passing through the short diagonal of the basal net. Adjacent sheets associate via a network of sodium ions and water molecules embedded between them. The morphology of sodium beijeran in the solid state is consistent with its observed rheological properties.

Keywords: Beijeran; Bacterial polysaccharide; X-ray diffraction; Three-dimensional structure

1. Introduction

Microbial polysaccharides are of great industrial interest because of their low production cost and sometimes unique or superior functional properties. For example, xanthan and gellan, from *Xanthomonas campestris* and *Pseudomonas elodea*, respectively, are well known in various food and non-food applications.[1] Pullulan and curdlan have been used extensively in the food industry in Japan for their useful properties such as gelation, high viscosity, and film formation.[2,3]

Beijeran is an anionic polysaccharide excreted by the soil bacterium *Azotobacter beijerinckii* YNM1.[4] The deacetylated polymer is found to form gels in aqueous solution in the presence of divalent ions, such as calcium and zinc. It also has the ability for film formation and exhibits pH-independent viscosity, and high water-holding capability under various humidity conditions.[5,6] All of these properties, along with the ease of production in large quantities, give beijeran a great potential for utilization in food, cosmetic, and pharmaceutical industries.

The chemical structure of beijeran was determined by NMR and chemical analysis.[5] The linear polysaccharide consists of a trisaccharide repeating unit, →3)-α-D-GalA-(1→3)-β-L-Rha-(1→3)-α-D-Glc-(1→ (or *–A–B–C–*) after removal of the acetyl groups in the native material. A monoclinic unit cell ($a = 12.77$, $b = 16.11$, c (fiber axis) $= 24.73$ Å and $\gamma = 96.8°$), large enough to accommodate four twofold helices of beijeran, was proposed from a preliminary X-ray and modeling analysis.[7] In search of the precise molecular morphology and the preferred interactions among the polymer chains, cations and other guest molecules that could be correlated with the functional properties, we have recently re-examined the X-ray data and found that a smaller unit cell, roughly half the original size, could lead us to the three-dimensional structure. The results of this new study are the topic of this article.

2. Experimental

Sample preparation.—Beijeran powder in its deacetylated form was provided by the Development Department of Tayca Co., Osaka, Japan. Oriented films were prepared as described earlier.[8] Sodium salt of the films were obtained by converting them first into the acid form by dipping in an acid solution (5:1 EtOH–1 M

* Corresponding author. Tel.: +1-765-4944923; fax: +1-765-4947953.
E-mail address: chandra@purdue.edu (R. Chandrasekaran).

0008-6215/02/$ - see front matter
PII: S0008-6215(01)00324-X

HCl), followed by neutralization using an NaOH solution (3:1 MeOH–1 M NaOH). A strip of the film was stretched to twice its original length in 75% aq 2-propanol at 60 °C and then annealed at 160 °C in the same medium. Film density was measured by the flotation method in a carbon tetrachloride-*m*-xylene solution at 30 °C.

X-ray data acquisition.—Diffraction patterns were recorded on photographic films in a pinhole camera on a microfocus X-ray generator. The pattern shown in Fig. 1 was chosen for structure analysis. All the Bragg reflections could be indexed on a monoclinic unit cell of dimensions $a = 12.72(6)$, $b = 11.41(8)$, c (fiber axis) = 24.62(9) Å and $\gamma = 123.7(3)°$. The meridional reflections on the second and sixth layer lines imply that beijeran has twofold helix symmetry. According to the measured film density (1.47 g/cc), the unit cell has room for four trisaccharide repeats, as well as four sodium ions and 34 water molecules.

Intensities of the reflections were measured with a Joyce Loebl Mark III microdensitometer. They were converted into observed structure amplitudes after applying Lorentz and polarization corrections.[9] Twenty-six out of 62 reflections within the field of view, up to 2.6 Å resolution, were too weak to be seen. The lowest measured intensity was assigned as the threshold value for each of them. A weak reflection was included in the structure refinement if its F_c was greater than F_o, but omitted otherwise.

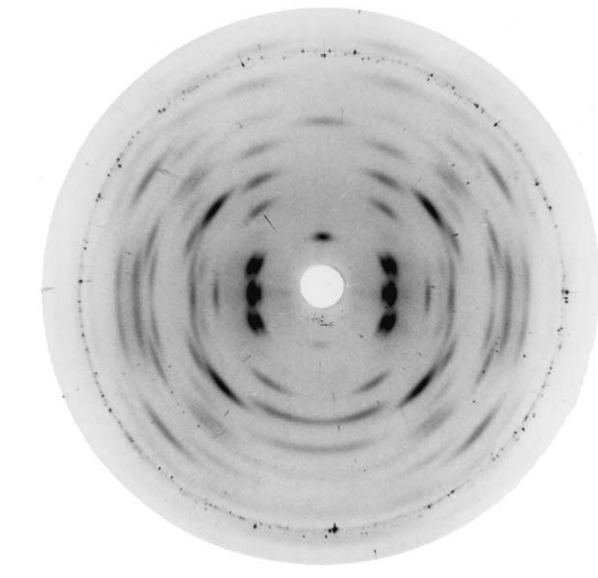

Fig. 1. X-ray diffraction pattern from a polycrystalline and oriented specimen of the sodium salt of beijeran using Cu K_α radiation of wavelength 1.5418 Å. The fiber is tilted from the vertical direction by 14°. The ring corresponds to 3.035 Å spacing characteristic of calcite.

3. Structure analysis

Model building and refinement.—The linked-atom least-squares (LALS) program[10] was used in the generation and refinement of the crystal structure. The function minimized in the least-square procedure is given by

$$\Omega = \sum w_m \Delta F_m^2 + \sum k_i \Delta c_i^2 + \sum e_j \Delta \theta_j^2 + \sum \lambda_h G_h$$

$$= \quad X \quad + \quad C \quad + \quad E \quad + \quad L$$

The terms X and C optimized the model against the X-ray data and non-bonded, as well as hydrogen bonding interactions, respectively; E retained the varied conformation angles and related parameters near standard or expected domains; and L ensured that constraints on helix symmetry and ring closure were fully satisfied.

First the beijeran helix was generated as a twofold helix of pitch 24.62 Å. The preferred chair conformations for the pyranosyl rings, $^1C_4$ in B, and $^4C_1$ in A and C, were incorporated in the model. While the six major conformation angles (ϕ_1, ψ_1), (ϕ_2, ψ_2), and (ϕ_3, ψ_3), control the helix geometry, three other angles, χ_A, χ_B and χ_C define the orientations of the carboxylate, methyl, and hydroxymethyl groups, respectively. Two-dimensional, hard-sphere maps[11] for the three disaccharide units, GalA-Rha, Rha-Glc and Glc-GalA, were computed for determining the allowed domains of the main-chain conformation angles. The centers of these domains were adopted as the starting values for building the helix. The bond angles at the glycosidic bridge oxygen atoms were initially set at the expected value of 116.5°.

After generating a stereochemically satisfactory helix whose diameter was more than 10 Å, the packing of two of them, one at the corner and another at the center, in the unit cell was investigated. This was set up to be consistent with the space group $P2_1$ (c-axis unique). Of the two cases considered, model P used the same polarity for both the helices, but they were aligned antiparallel in model A. In each case, the packing parameters were (μ_1, 0, 0, 0) for the first and (μ_2, 1/2, 1/2, w_2) for the second helix, μ being its orientation relative to the a^*-axis, and w its fractional translation along the c-axis from the ab-plane. The task was to determine the preferred mode including the most probable values for μ_1, μ_2 and w_2. These were evaluated as follows: treating the helix as a rigid body, both the crystallographic R-value ($= \Sigma||F_o| - |F_c||/\Sigma|F_o|$) and intermolecular contacts in the three-dimensional space were examined at intervals of 5° for μ_1 and μ_2, and 0.02 for w_2. Those domains exhibiting fewer short contacts and low R-values were selected and subjected to detailed X-ray refinement in which both the molecular and packing parameters were allowed to vary. This enabled us to narrow down the number of competing alternatives.

Table 1
Cartesian and cylindrical polar atomic coordinates of a repeating unit of the beijeran helix, and those of cations and water molecules in an asymmetric unit

Group	Atom	x (Å)	y (Å)	z (Å)	r (Å)	ϕ (°)
Galacturonate (*A*)	C-1	1.018	1.038	9.555	1.454	45.55
	C-2	0.482	0.203	10.710	0.523	22.79
	C-3	−0.887	0.706	11.142	1.133	141.49
	C-4	−0.832	2.199	11.436	2.351	110.73
	C-5	−0.219	2.945	10.256	2.954	94.26
	C-6	−0.032	4.422	10.532	4.422	90.42
	O-1	0.121	0.952	8.498	0.960	82.73
	O-2	0.416	−1.162	10.312	1.235	−70.29
	O-3	−1.310	0.000	12.310	1.310	180.00
	O-4	−0.038	2.449	12.594	2.449	90.90
	O-5	1.078	2.410	9.951	2.640	65.90
	O-61	0.748	4.732	11.458	4.791	81.01
	O-62	−0.672	5.219	9.813	5.262	97.34
	H-1	2.027	0.689	9.287	2.141	18.79
	H-2	1.179	0.260	11.559	1.207	12.45
	H-3	−1.597	0.519	10.323	1.679	162.00
	H-4	−1.850	2.574	11.619	3.170	125.70
	H-5	−0.873	2.843	9.377	2.974	107.08
Rhamnose (*B*)	C-1	1.406	1.223	5.019	1.863	41.01
	C-2	1.023	0.580	6.346	1.176	29.56
	C-3	0.482	1.627	7.309	1.697	73.49
	C-4	−0.686	2.344	6.646	2.442	106.31
	C-5	−0.196	2.988	5.341	2.994	93.75
	C-6	−1.296	3.691	4.567	3.912	109.34
	O-1	1.846	0.219	4.141	1.859	6.77
	O-2	0.045	−0.417	6.075	0.419	−83.81
	O-3	0.121	0.952	8.498	0.960	82.73
	O-4	−1.198	3.328	7.540	3.537	109.79
	O-5	0.323	1.963	4.477	1.989	80.64
	H-1	2.267	1.890	5.170	2.952	39.81
	H-2	1.906	0.096	6.788	1.908	2.89
	H-3	1.281	2.351	7.526	2.678	61.41
	H-4	−1.481	1.618	6.421	2.194	132.47
	H-5	0.598	3.715	5.566	3.763	80.85
	H-61	−1.859	4.348	5.246	4.729	113.15
	H-62	−0.850	4.292	3.761	4.375	101.21
	H-63	−1.975	2.942	4.134	3.544	123.88
Glucose (*C*)	C-1	2.565	−0.326	0.498	2.586	−7.25
	C-2	2.422	−0.669	1.975	2.513	−15.43
	C-3	1.844	0.510	2.743	1.913	15.47
	C-4	2.664	1.766	2.478	3.197	33.54
	C-5	2.814	1.991	0.977	3.447	35.28
	C-6	3.716	3.161	0.649	4.878	40.39
	O-1	1.310	0.000	0.000	1.310	0.00
	O-2	1.593	−1.817	2.113	2.417	−48.75
	O-3	1.846	0.219	4.141	1.859	6.77
	O-4	2.025	2.906	3.048	3.542	55.13
	O-5	3.392	0.831	0.358	3.492	13.77
	O-6	3.439	4.292	1.474	5.500	51.30
	H-1	3.027	−1.172	−0.032	3.246	−21.18
	H-2	3.408	-0.928	2.388	3.532	−15.23
	H-3	0.810	0.669	2.402	1.051	39.56
	H-4	3.660	1.657	2.933	4.017	24.35
	H-5	1.825	2.188	0.536	2.849	50.16

Table 1 (*Continued*)

Group	Atom	x (Å)	y (Å)	z (Å)	r (Å)	ϕ (°)
	H-61	3.567	3.455	−0.401	4.966	44.09
	H-62	4.765	2.870	0.803	5.563	31.06
Sodium	Na-1	0.410	6.142	1.111	6.155	86.18
	Na-2	3.380	6.454	3.296	7.285	62.35
Water	*W*-1	3.767	6.290	−1.345	7.332	59.08
	W-2	7.643	−1.644	3.044	7.817	−12.14
	W-3	6.813	−4.329	3.205	8.072	−32.43
	W-4	8.302	2.144	7.031	8.575	14.48
	W-5	9.101	1.017	9.622	9.158	6.38
	W-6	7.220	−4.387	9.453	8.448	−31.28
	W-7	2.588	7.430	0.971	7.868	70.80
	W-8	4.835	−1.885	7.080	5.189	−21.30
	W-9	4.626	−0.837	9.651	4.701	−10.26
	W-10	0.392	5.283	7.186	5.298	85.76

The cylindrical coordinates of the next trisaccharide in the helix are (r, $\phi+180°$, $z+c/2$). For a down-pointing helix, the coordinates are (r, $-\phi$, $-z$). The packing parameters are:

Molecule	Sense	μ (°)	u	v	w
Helix I	up	-1.8	0.0	0.0	0.0
Helix II	down	29.2	0.5	0.5	0.19
Na and water		0.0	0.0	0.0	0.0

Table 2
Observed and calculated structure amplitudes for sodium beijeran

h k	l								
	0	1	2	3	4	5	6	7	8
0 0	M [*712*]	N [*0*]	M [*7*]	N [*0*]	M [*7*]	N [*0*]	M [*58*]	N [*0*]	M [*129*]
-1 1 1 0	100 *95*	112 *119*	35 *39*	82 *84*	97 *87*	81 *87*	55 *59*	85 *68*	94 *96*
0 1	174 *118*	135 *95*							
-2 1	86 *80*	(50) (*62*)	[52] [*40*]	198 *135*	[59] [*45*]	66 *70*	[67] [*47*]	(72) (*82*)	[76] [*47*]
1 1 -1 2	(55) (*70*)	72 *94*	65 *83*	[61] [*45*]	127 *175*	90 *88*	97 *84*	104 *93*	108 *88*
2 0 -2 2	116 *113*	90 *92*	118 *189*	76 *70*					
0 2	[66] [*54*]	(67) (*153*)	(69) (*109*)	[71] [*21*]	(75) (*78*)	[78] [*42*]	[82] [*54*]	[87] [*62*]	[91] [*48*]
-3 1 -3 2	98 *77*	130 *89*	138 *137*	86 *78*	*180* *123*	102 *89*	91 *101*		
2 1 -2 3	176 *126*	187 *182*	[85] [*50*]	[87] [*39*]	(90) (*107*)	[93] [*53*]	[97] [*58*]		
1 2 -1 3	[87] [*48*]	[87] [*46*]							
3 0 -3 3	142 *142*	153 *125*							
-4 2 0 3	[99] [*63*]	[100] [*66*]							

In each reflection box, the observed amplitude is given in the first line and the calculated (*italic*) in the second. The curved and rectangular brackets refer to below threshold reflections included in, and rejected from, the least-squares refinement, respectively. M and N denote respectively meridional and systematically absent reflections. The calculated structure amplitudes include a temperature factor with $B = 6.0$ Å^2.

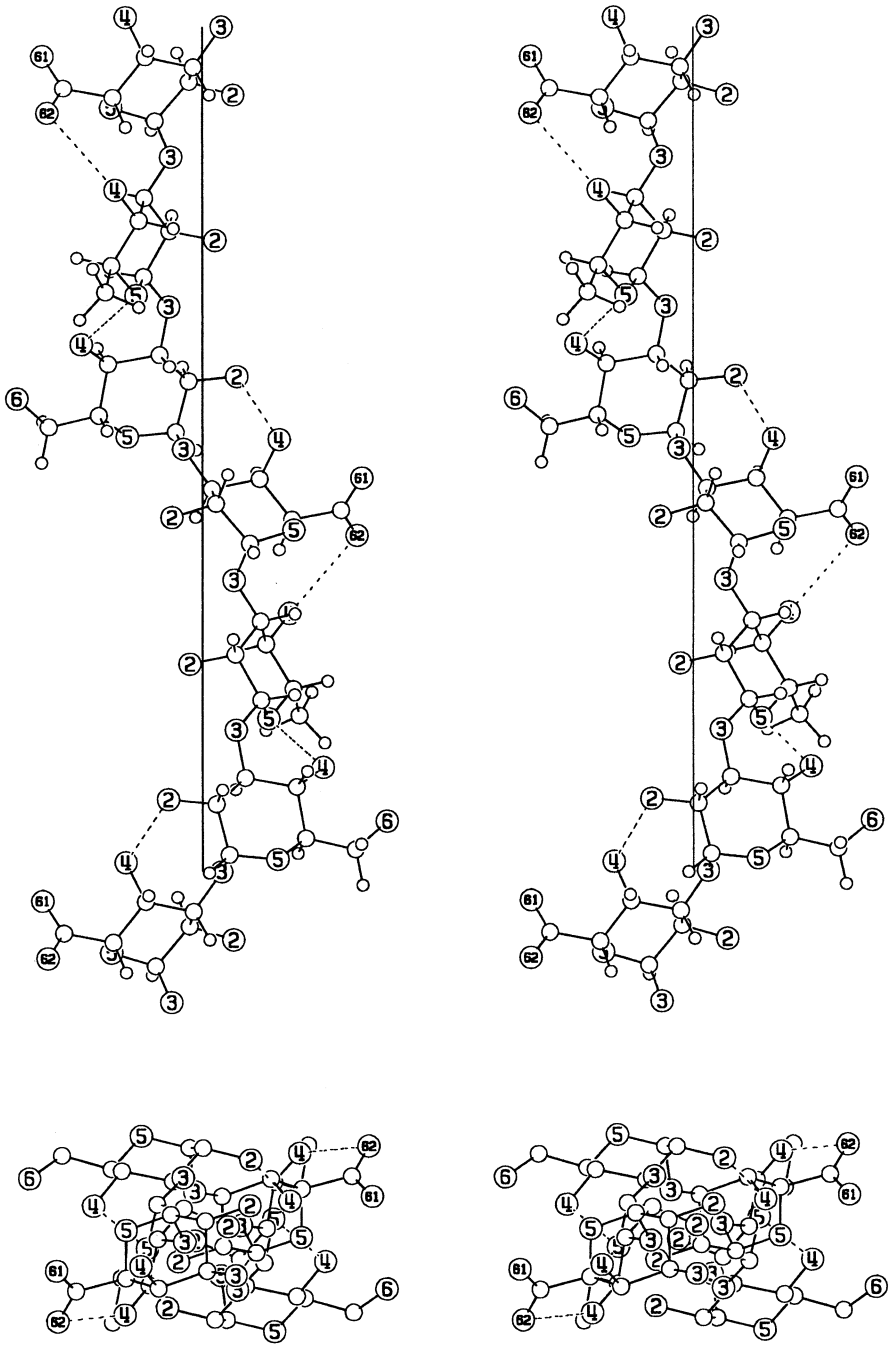

Fig. 2. Two mutually perpendicular stereo views of the beijeran helix: (Top) More than a turn normal to the helix axis (vertical line). All hydrogen atoms are included only in this panel. Hydrogen bonds are drawn in dashed lines. (Bottom) One turn down the helix axis. The numbers correspond to oxygen atoms of selected functional groups.

Three-dimensional difference electron density maps were subsequently computed, using normal atomic scattering factors, for half of the unit cell, i.e., the crystallographic asymmetric unit ($z = 0$ to $c/2$), and examined carefully for verification of the chosen structure. The surroundings were searched for cations and water molecules. Addition of guest molecules in augmenting the crystal structure was always subject to lowering of the R-value. In order to compensate for the intractable water molecules, water smeared atomic scattering factors[12] were used in computing the R-values.

The final choice.—At the outset, the unit cell appeared to be too small to contain two sinuous helices, but we found later that this could be managed with some effort. We could obtain several combinations of the packing variables leading to satisfactory intermolecular contacts when the helices were aligned parallel (either both up or both down). Unfortunately, with the

R-value always higher than 0.50, none of them matched well the observed X-ray data. Meanwhile, we discovered from the computer search that there was only one narrow domain for the antiparallel arrangement having good contacts and a much lower R-value, 0.36. Model A was therefore adopted for further analysis.

The difference Fourier map confirmed that both the molecular geometry selected, and the mode of packing used were correct. There were seven extra positive peaks in the map, which were identified as potential guest molecules. Upon including them as water in the crystal structure one at a time and refining their positions, the R-value decreased to 0.27. Difference map for the augmented structure helped to identify five more guest molecules. This further lowered the R-value to 0.21. To find out which guest molecules were sodium ions, we examined the peaks near the carboxylate groups. Only two of them were found to have four or more oxygen atoms as ligands with relatively smaller bonding distances. Re-labeling these two as sodium ions resulted in R dropping to 0.20. A final round of refinement of the molecular, as well as packing parameters in the crystal structure, in which the bond angles at the bridge oxygen atoms were also varied, improved the X-ray fit further ($R = 0.19$). This accounts for the 36 observed and seven out of 26 unobserved reflections. With very small changes in the varied parameters, the refinement was deemed complete and concluded. A difference map at this stage was featureless suggesting that the seven out of 17 water molecules per asymmetric unit that we could not find were most probably amorphous. All the non-bonded contacts in the structure are at or above the acceptable limits.[11] The final atomic coordinates are given in Table 1. The observed and calculated structure amplitudes are listed in Table 2.

4. Results

Helix geometry.—The beijeran molecule forms a twofold helix as shown in Fig. 2. Since it has a trisaccharide repeat, the polymer chain spirals around the molecular axis with a right-handed twist as seen in the top panel. This is achieved by a concerted effort among the three pairs of quite distinct glycosidic conformation angles listed in Table 3. Although all the linkages are of the same type (1→3), the bond configurations (*a*, *e*), (*a*, *e*) and (*e*, *e*), where *a* and *e* stand for axial and equatorial, respectively, are quite distinct. Consequently, the polymer forms an extended structure unlike any other in the literature. Two important features can be inferred from Fig. 2 by using the bridge oxygen atoms for reference. The first is that a trisaccharide repeat is on one side of the helix axis such that successive monomers are evenly spaced (4.0 Å apart) in the z-direction, and its helix mate is on the other side. The second is that the 180° twist per repeat is unevenly distributed: 97° for GalA, 76° for Rha, but only 7° for Glc. As a result, there is a sharp turn at the junction between adjacent repeats.

Table 3
Major conformation and bridge bond angles (and e.s.d.) in °

Parameter	Angle	Location
ϕ_1 (O-5–C-1–O-3–C-3)	115(2)	*C*-(1→3)-*A*
ψ_1 (C-1–O-3–C-3–C-4)	60(3)	*C*-(1→3)-*A*
τ_1 (C-1–O-3–C-3)	116.4(1)	*C*-(1→3)-*A*
χ_A (C-4–C-5–C-6–O-61)	63(6)	carboxylate
ϕ_2 (O-5–C-1–O-3–C-3)	64(3)	*A*-(1→3)-*B*
ψ_2 (C-1–O-3–C-3–C-4)	−139(4)	*A*-(1→3)-*B*
τ_2 (C-1–O-3–C-3)	116.5(1)	*A*-(1→3)-*B*
χ_B (C-4–C-5–C-6–H-61)	49(9)	methyl
ϕ_3 (O-5–C-1–O-3–C-3)	37(1)	*B*-(1→3)-*C*
ψ_3 (C-1–O-3–C-3–C-4)	56(3)	*B*-(1→3)-*C*
τ_3 (C-1–O-3–C-3)	117.8(1)	*B*-(1→3)-*C*
χ_C (C-4–C-5–C-6–O-6)	−44(6)	hydroxymethyl

The molecular surface is the site of the carboxylate, methyl, and hydroxymethyl groups and they define the helix diameter at about 11.0 Å. Atoms O-2 and O-3 are aligned in the interior at only 0.4 Å from the helix axis. As a result, the helix projects as a rectangle (Fig. 2, bottom panel) of sides 9.8 and 5.6 Å.

The flexibility of the helix is tempered by three hydrogen bonds per repeat between successive monomers across the glycosidic oxygen atoms. These are labeled ***1***–***3*** in Table 4 where a series of attractive interactions (less than 3.1 Å) between non-bonded atoms in the crystal structure are listed. While the carboxylate group is the acceptor in the first hydrogen bond, the glucose hydroxyl groups are the donors in the other two. Helices I and II are antiparallel, separated by only 5.72 Å along the short diagonal of the basal plane. The resulting tight fit facilitates four sets of helix–helix hydrogen bonds (***4*** through ***7*** in Table 4) pictured in Fig. 3(a). Since the dyad relating them is not perpendicular (8° away) from the line of separation between the helices, the interactions from I to II are not exactly the same as those from II to I. It is noticed that atom O-4*C* in ***3*** is also involved as a bifurcated donor in ***6***. In contrast, atom O-6*C* is a bifurcated donor for two interchain hydrogen bonds in ***7***. The other pairs of helices in the lattice are too far apart to interact directly.

Cations and water molecules.—The space between the helices II and the *a*-translation mate of I, which are 10.64 Å apart along the long diagonal of the basal plane is the site of the guest molecules in this structure. One sodium ion near the carboxylate group and five

Table 4
Attractive interactions among beijeran helices, sodium ions, and water molecules

Type	No.	Atom *X*	Atom *Y*	Precursor *P*	*X*···*Y* (Å)	*P*-*X*···*Y* (°)
Intrahelix	***1***	O-4*B*	O-62*A*	C-4*B*	3.00	148
	2	O-2*C*	O-4*A*	C-2*C*	2.48	120
	3	O-4*C*	O-5*B*	C-4*C*	2.41	104
Interhelix	***4***	O-4*A*(I)	O-4*C*(II)	C-4*A*	2.78	152
		O-4*A*(II)	O-4*C*(I)	C-4*A*	2.85	148
	5	O-2*B*(I)	O-5*C*(II)	C-2*B*	2.76	146
		O-2*B*(II)	O-5*C*(I)	C-2*B*	3.06	118
	6	O-4*C*(II)	O-61*A*(I)	C-4*C*	2.93	130
	7	O-6*C*(I)	O-4*A*(II)	C-6*C*	2.98	125
		O-6*C*(I)	O-2*C*(II)	C-6*C*	2.50	102
Sodium coordination	***8***	O-61*A*(I,01)	Na-1	C-6*A*	2.42	108
		O-4*A*(I,01)	Na-1	C-4*A*	2.97	107
		O-6*C*(II,-10)	Na-1	C-6*C*	2.41	153
		O-4*C*(II,-10)	Na-1	C-4*C*	2.99	123
		W-7	Na-1		2.53	
	9	O-61*A*(II)	Na-2	C-6*A*	2.52	111
		O-4*A*(II)	Na-2	C-4*A*	2.50	115
		O-6*C*(I)	Na-2	C-6*C*	2.92	173
		W-7	Na-2		2.64	
Water bridges	***10***	*W*-6	*W*-1		2.91	
		W-7	*W*-1		2.84	
		W-9	*W*-1		2.78	
		O-4*B*(I,10)	*W*-6	C-4*B*	3.05	119
		O-4*B*(II,0-1)	*W*-6	C-4*B*	2.85	110
		O-2*C*(I,01)	*W*-7	C-2*C*	2.62	110
		O-2*B*(II)	*W*-9	C-2*B*	3.03	84
		W-8	*W*-9		2.78	
		O-62*A*(II,0-1)	*W*-8	C-6*A*	2.89	138
		O-2*A*(II)	*W*-8	C-2*A*	2.95	135
	11	O-2*A*(II)	*W*-4	C-2*A*	3.07	101
		O-5*C*(II)	*W*-4	C-5*C*	2.90	96
		O-2*B*(I,11)	*W*-4	C-2*B*	3.08	150
		W-5	*W*-4		2.94	
		O-62*A*(I,10)	*W*-5	C-6*A*	3.01	144
		O-2*A*(I,11)	*W*-5	C-2*A*	2.93	145
	12	O-4*C*(II)	*W*-2	C-4*C*	2.80	123
		W-2	*W*-3		2.81	
		O-2*C*(II,0-1)	*W*-3	C-2*C*	2.81	92
	13	O-62*A*(I)	*W*-10	C-6*A*	2.78	113
		O-4*B*(I)	*W*-10	C-4*B*	2.45	105
		O-61*A*(II)	*W*-10	C-6*A*	2.63	93

I and II in parentheses refer to the two helices in the unit cell, the second and third digits, if any, refer to *a*- and *b*-translations.

water molecules per trisaccharide repeat of I, and a similar number for II have been tracked. The cations Na-1 (***8***) and Na-2 (***9***) balance the charge on the carboxylate groups, and the water molecules *W*-1 though *W*-10 establish a series of water bridges (***10*** through ***13***) between neighboring helices in an intricate way. As shown in Fig. 3(b), Na-1 binds the carboxylate atom O-61 of I (***8***) and likewise Na-2 in II (***9***). In each case, the ion also finds two or three oxygen atoms in the polymer chains as ligands. Additionally, *W*-7 is an important common ligand to both the ions. The result is that the beijeran helices associate primarily by carboxylate–sodium–water–sodium–carboxylate interactions, similar to that observed in the case of gellan.[13]

The unit cell contains two beijeran helices of opposite polarity. The packing arrangement in the monoclinic lattice (Fig. 4) illustrates vividly that the helices, 5.62 Å apart, are very tightly packed along the short diagonal.

The direct contacts between their functional groups (***4***–***7***) result in polymer sheet formation in the (−110) plane. The distance between sheets is 10.64 Å along the long diagonal. Sodium ions and water molecules occupy the void between the sheets and hold them together.

5. Discussion

Due to lack of structural data on polymers of related sequence, it is not possible to compare the main chain conformation angles of beijeran with any others. It is satisfying to note that that the backbone conformation

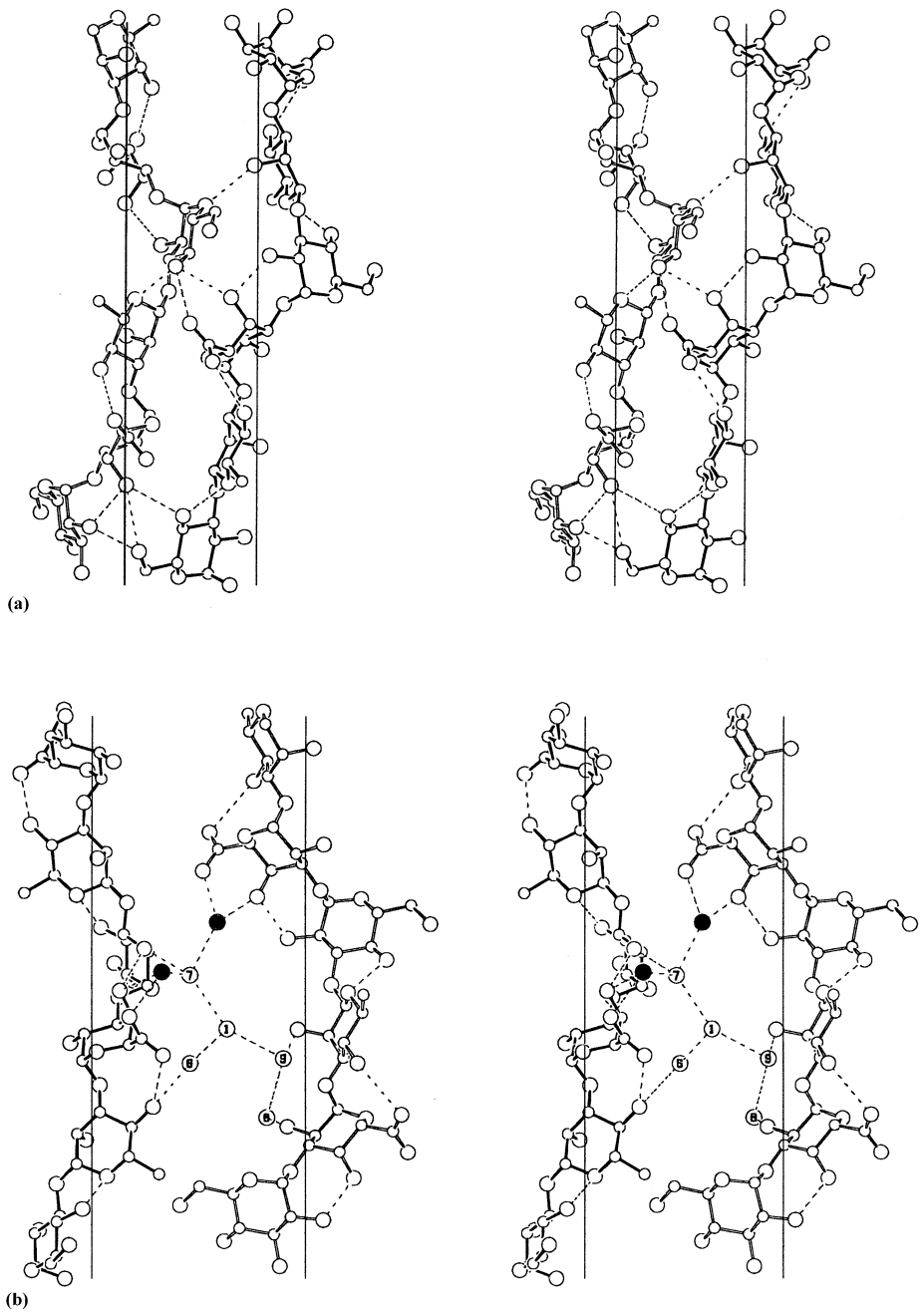

Fig. 3. Interhelical interactions in the unit cell shown in stereo: (a) Helix II on the left is antiparallel to helix I on the right. They are 5.72 Å apart along the short diagonal of the basal plane and connected by a series of hydrogen bonds (dashed lines). (b) Helix I on the left is antiparallel to helix II on the right. They are 10.64 Å apart along the long diagonal of the basal plane and are connected at their carboxylate groups by sodium–water–sodium bridges. The ions are shown as filled circles and water molecules are numbered.

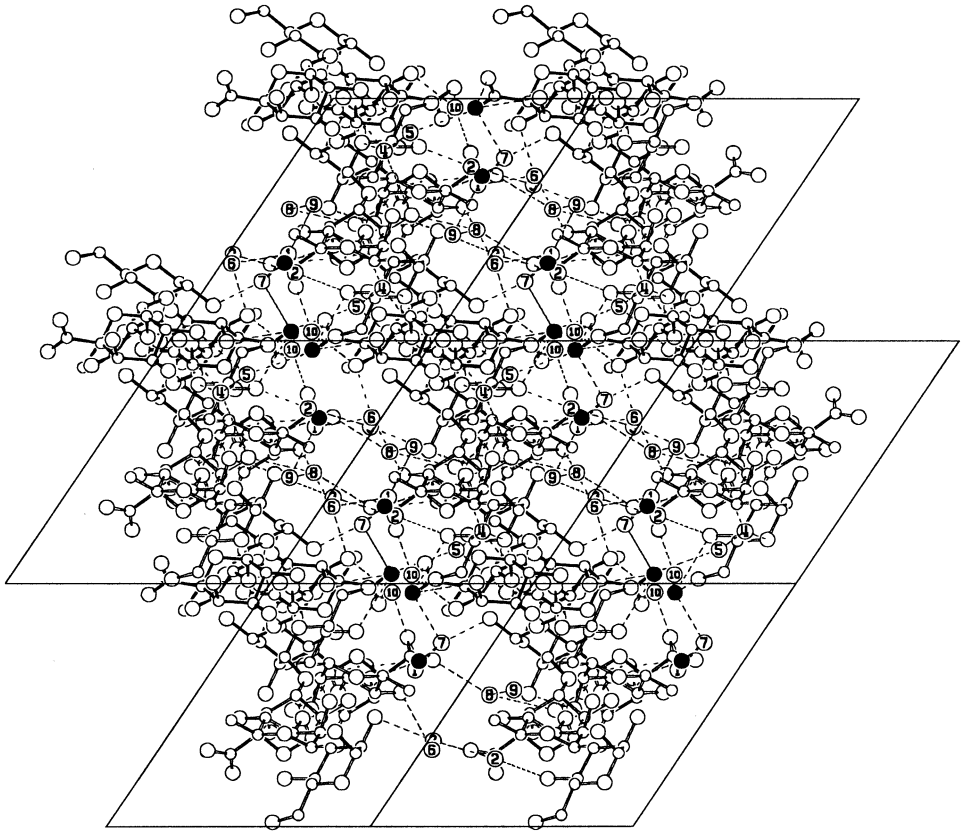

Fig. 4. Packing arrangement of helices in the monoclinic lattice. Seven unit cells shown in the *c*-axis projection highlight the formation of sheets along the short diagonal. Water molecules (numbered) and sodium ions (filled circles) hold the sheets together by hydrogen bonds and ionic interactions.

angles (Table 3) are within 10° for ψ_1 and ϕ_2, and about 40° away for the other four, from the molecular model A1A2B3 deduced from *n*–*h* plot and energy calculations.[14] This feature might be attributed to the packing forces. The side group conformations are not out of the ordinary. The hydroxymethyl group of the glucopyranosyl unit stays in the same gauche minus domain as is the case for the (1→3)-linked glucosyl unit in the gellan family polysaccharides. To some extent, the carboxylate group orientation ($\chi_A = 63°$) differs from those in the gellan family (-8 to 37°).[15] This change is apparently necessary for facilitating the O-4*B*···O-62*A* hydrogen bond that contributes to the structural rigidity of the beijeran helix.

Formation of sheets is a common phenomenon in some simple polysaccharide structures, such as cellulose, mannan and chitin (water insoluble), and galactomannan (water soluble), to name a few.[15] Now beijeran, a more complex structure, joins this list. As already stated, the most remarkable feature of the crystal structure is the formation of a thick sheet in the (-110) plane. Beijeran molecules are tightly nestled leaving no room for any guest molecule to sit in or pass through this polymer sheet. As seen in Fig. 4, all the sodium ions and water molecules are embedded between the sheets and none elsewhere. Together, they glue the sheets to form a well-knitted network. This could explain beijeran's abilities for water holding and formation of oxygen-impervious films.

In anionic polysaccharides, carboxylate–carboxylate interactions mediated by ions and water molecules are usually a major factor for the association of helices and their details may be used to correlate with the observed rheological properties. In sodium beijeran, the ion–water–ion-bridge and several water-mediated interactions among the polymer chains constitute a major force of attraction between the polysaccharide sheets. However, this seems to be overpowered by the hydrogen-bonded association of polymer chains within the sheets. In other words, the interactions within the sheets are stronger than those between them. Thus, the formation of a sheet structure might explain why the viscosity of beijeran solution is stable over a wide range of pH from 2 to 12.[6] For the same reason, it is equally understandable why sodium beijeran does not gel. It will therefore be interesting to see how divalent ions would affect the beijeran packing arrangement that could explain gel formation.

Acknowledgements

This research was supported by the Industrial Consortium of the Whistler Center for Carbohydrate Research. We thank Professor Akira Misaki for providing some beijeran samples and related information.

References

1. Kang, K. S.; Pettitt, D. J. In *Industrial Gums. Polysaccharides and their Derivatives*; Whistler, R. L.; BeMiller, J. N., Eds. Xanthan, Gellan, Welan, and Rhamsan, 3rd ed.; Academic: New York, 1993; pp. 341–397.
2. Tsujisaka, Y.; Mitsuhashi, M. In *Industrial Gums. Polysaccharides and their Derivatives*; Whistler, R. L.; BeMiller, J. N., Eds. Pullulan, 3rd ed.; Academic: New York, 1993; pp. 447–460.
3. Harada, T.; Teasaki, M.; Harada, A. In *Industrial Gums. Polysaccharides and their Derivatives*; Whistler, R. L.; BeMiller, J. N., Eds. Curdlan, 3rd ed.; Academic: New York, 1993; pp. 427–445.
4. Oiso, Y.; Okumiya, T.; Sugihara, R.; Nakanishi, O.; Nakagawa, M.; Otani, K.; Misaki. A. *Abstracts of Papers, XV Japanese Carbohydrate Symposium*, Sendai, Japan, July 1993; pp. 115–116.
5. Oiso, Y.; Okumiya, T.; Kawashima, K.; Sone, Y.; Kakuta, M.; Misaki, A. *Abstracts of XVII Japanese Carbohydrate Symposium*, Kyoto, Japan, July 1995; pp. 89–90.
6. Misaki, A.; Oiso, Y.; Kakuta, M.; Sone, Y.; Ogawa, K. *Abstracts of XVIII International Carbohydrate Symposium*, Mirano, Italy, July 1996; pp. 651.
7. Ogawa, K.; Yui, T.; Nakata, K.; Kakuta, M.; Misaki, A. *Carbohydr. Res.* **1997**, *300*, 41–45.
8. Ogawa, K.; Yui, T.; Nakata, K.; Nitta, Y.; Kakuta, M.; Misaki, A. *Biosci. Biotech. Biochem.* **1996**, *60*, 551–553.
9. Chandrasekaran, R.; Stubbs, G. In *International Tables for Crystallography*, *Crystallography of Biological Macromolecules*; Rossmann, M. G.; Arnold, E., Eds. Fiber Diffraction; Kluwer Academic: Dordrecht, 2001; Vol. F, pp. 444–450.
10. Smith, P. J. C.; Arnott, S. *Acta Crystallogr., Sect. A* **1978**, *34*, 3–11.
11. Ramachandran, G. N.; Sasisekharan, V. *Adv. Prot. Chem.* **1968**, *23*, 283–437.
12. Chandrasekaran, R.; Radha, A. *J. Biomol. Struc. Dynam.* **1992**, *10*, 153–168.
13. Chandrasekaran, R.; Puigjaner, L. C.; Joyce, K. L.; Arnott, S. *Carbohydr. Res.* **1988**, *181*, 23–40.
14. Yui, T.; Nabekura, T.; Ogawa, K. *Carbohydr. Res.* **1997**, *304*, 341–345.
15. Chandrasekaran, R. *Adv. Carbohydr. Chem. Biochem.* **1997**, *52*, 311–439.